Role of glide systems in channel die compression of commercially pure titanium alloy

A Chattopadhyay, L Bao, J-S Lecomte, Y D Zhang, C Schuman, M-J Philippe, C Esling

Role of glide systems in channel die compression of commercially pure titanium alloy

A. Chattopadhyay[*1,2], L. Bao[1,3], J.-S. Lecomte[1], Y. D. Zhang[1], C. Schuman[1], M.-J. Philippe[1] and C. Esling[1]

[1]*LEM3-UMR 7239, Laboratoire d'Etude des Microstructures et de Mécanique des Matériaux, University of Metz, Metz 57045, France*

[2]*Research and Development, Tata Steel Limited, Jamshedpur 831007, India*

[3]*Key Laboratory for Anisotropy and Texture of Materials (Ministry of Education), Northeastern University, Shenyang 110004, China*

**Corresponding author,* *email bhoda29@yahoo.co.in*

Abstract

Plastic deformation process of Ti alloys depends on the competition of active deformation modes: slip and twinning. The specific deformation mechanism depends on the availability of the specific deformation modes as well as on the critical resolved shear stress for slip and the twin activation stress. Effort has been made to provide information on the different slip systems other than prismatic slips, which get activated during the channel die compression process. It is found that, though at the initial stage of deformation, prismatic slip is prevalent, but other slip systems, especially pyramidal types, also appear at the later stage of deformation. Transmission electron microscopy results confirm the presence of pyramidal slips beside prismatic ones. It is also observed that twining does not take place in those grains having the most stable orientation as per the hexagonal close packed system. Information on the critical resolved shear stresses of different glide systems for T40 is also provided.

Keywords: *Ti alloy, Plastic deformation, EBSD, TEM, CRSS*

Introduction

The plastic deformation phenomenon of Ti alloys substantially depends on the competition of active deformation modes: slip and twinning. The specific deformation mechanism depends on the availability of specific deformation modes as well as on the critical resolved shear stress (CRSS) for slip and the twin activation stress [1,2]. Different slip and twin systems, which are possible in hexagonal material, are given in Table 1. For pure titanium, $\{10\bar{1}0\}\langle 11\bar{2}0\rangle$ slip (prismatic slip) is known to be responsible for the primary deformation.

This slip mode alone is not able to accommodate the imposed strain in the polycrystalline grains because it cannot provide five independent slip systems [3–7]. Additional deformation mechanisms, such as pyramidal planes with $\langle c + a \rangle$ Burger's vector or twinning, usually have to be activated. The observed ductility has been attributed essentially to the occurrence of twinning, notably the $\{1121\}$ tensile twinning and $\{1122\}$ compression twinning systems [8–10]. The present work aims to provide information, lacking in literature, on different slip systems other than prismatic slips, which get activated during channel die compression process, and prove their presence using transmission electron microscopy (TEM) technique. It also aims to provide information on CRSS of the different glide systems for T40.

Experimental

The as received hot rolled material, whose composition is Ti–3H–52C–41N–1062O–237Fe (wt ppm), is compressed in channel die to different levels. Before compression operation, the samples were mechanically ground and then electrolytically polished in a solution of 20 mL perchloric acid in 80 mL methanol at 17 V (30 s) and at the temperature of 5°C. Then, the samples were compressed under the channel die in three passes: 10, 20 and then 30% reduction. Before the compression process, two sheets are sandwiched and firmly stuck together to avoid any surface damage in order to maintain a good surface quality (Fig. 1a). To follow the rotation of the individual grains during the deformation, a specific area was carefully polished and marked out with four microindentations. The orientation of all the grains in this polished area (~200 grains) was measured by SEM/electron backscatter diffraction (EBSD) before and after each deformation step. The EBSD measurements were performed with a JEOL 6500F SEM with a step size of 0?2 mm. The average grain size of the material was ~80 mm. The slip systems are determined by trace analysis.

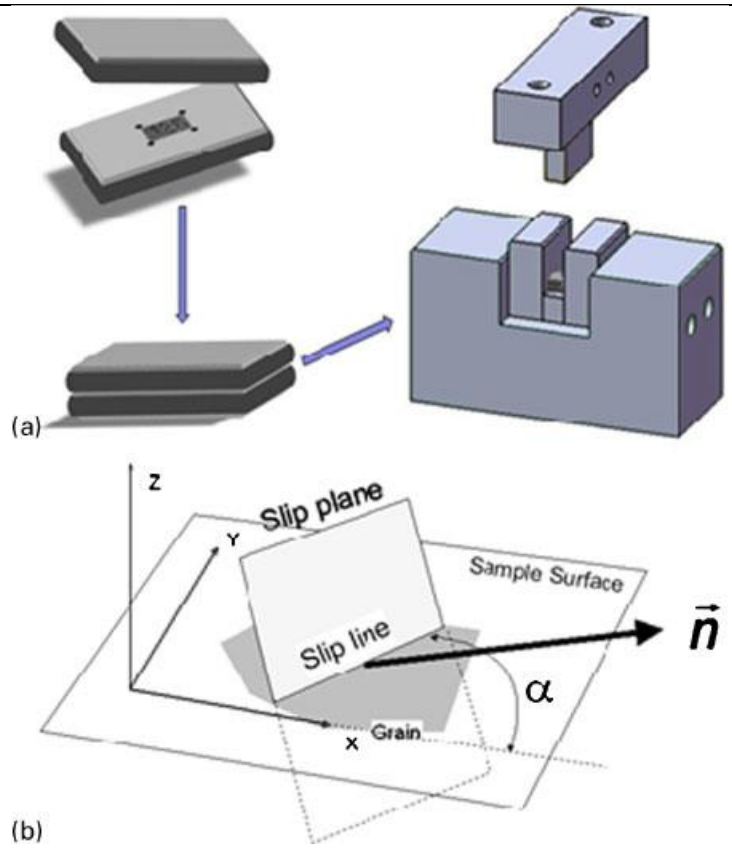

Fig 1 *a schematic of channel die compression operation on sandwich samples. Inner surface was initially polished, and orientation of grains was measured by EBSD before and after each compression step and b schematic of geometrical position of slip line on sample*

First, trace angles of all the possible slip plane traces on the sample surface with respect to the compression direction are calculated using the measured orientation of the grain concerned. Then, the trace angles of the observed slip plane traces are measured in the same coordinate system and compared with the calculated ones to conclude and identify the corresponding active slip system. It should be noted that$\{1\bar{1}01\}[11\bar{2}0]$ pyramidal 1<a> (π_1<a>) slip and $\{1\bar{1}01\}[11\bar{2}3]$ pyramidal 1<c+a> (π_1<c+a>) slip systems possess the same slip plane. The one showing the higher Schmid factor is selected. Therefore, by slip trace measurement, it is not possible to distinguish between pyramidal 1<a> and pyramidal 1<c+a>. The schematic diagram of the geometrical position of a slip line on the sample is shown in Fig. 1b. In order to confirm the obtained result statistically, for each stage of compression, >300 grains were analysed.

The glide system was studied using a TEM Philips CM20 operating at 200 keV [11,12]. The selected area diffraction (SAD) pattern is taken at a camera length of 880 mm.

Results and discussion

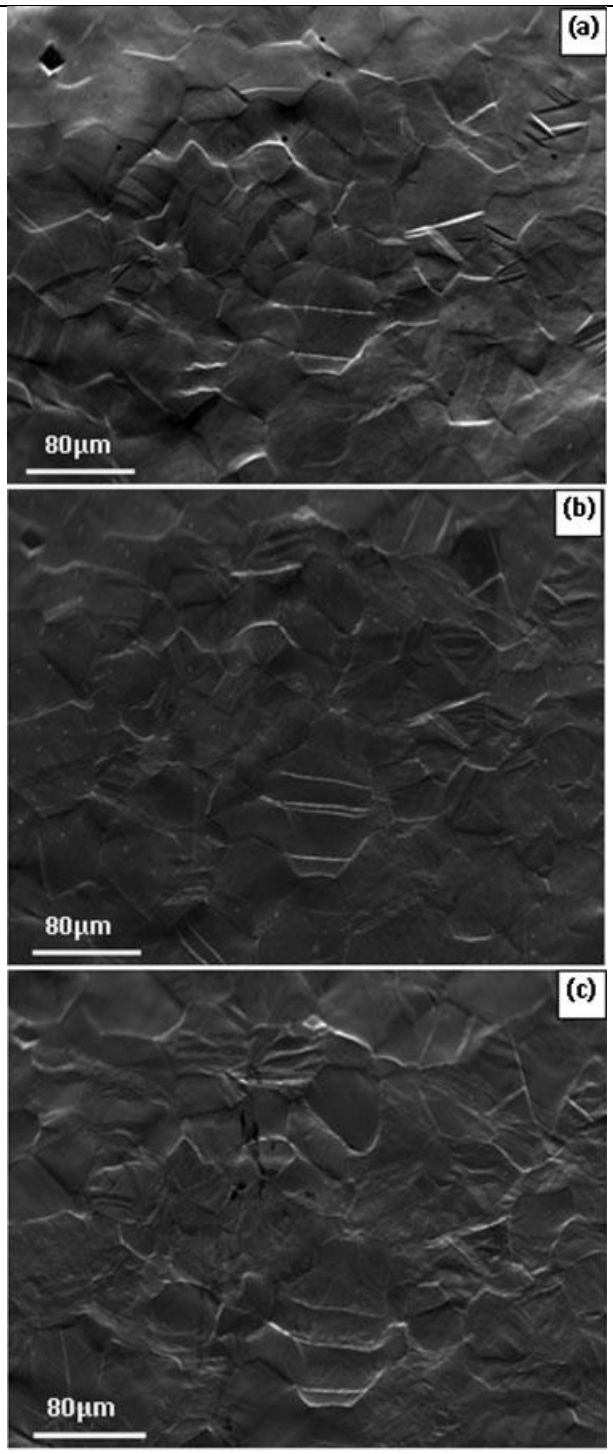

Fig. 2 *Field emission gun SEM microstructure of a 10%, b 20% and c 30% deformed sample*

The microstructure obtained after different stages of compression is given in Fig. 2. Traces of slips and twins can be observed there. The EBSD mapping results are given in Fig. 3. The results are obtained based on the Euler angle calculation. Twin boundaries are also included in the analysis. The red coloured twins are compressive $\{11\bar{2}2\}[\bar{1}\bar{1}23]$in nature, whereas blue indicates tension twins $\{10\bar{1}2\}[\bar{1}011]$If Fig. 2 can be observed sequentially, then in many grains the growth of either type of twin can be observed. In a few cases, it is marked inside the figure. In some other places, the generation of second order twins is also observed. These figures give direct idea about the microstructural evolution during the compression process.

Table 1 *List of different slip systems present in hexagonal close packed material*

Slip/twin	$\vec{b}$	Slip system	Notation
Basal	$\langle a \rangle$	$\{0002\}[11\bar{2}0]$	$B\langle a \rangle$
Prismatic	$\langle a \rangle$	$\{1\bar{1}00\}[11\bar{2}0]$	$P\langle a \rangle$
Pyramidal π_1	$\langle a \rangle$	$\{1\bar{1}01\}[11\bar{2}0]$	$\pi_1\langle a \rangle$
Pyramidal π_1	$\langle c+a \rangle$	$\{1\bar{1}01\}[11\bar{2}\bar{3}]$	$\pi_1\langle c+a \rangle$
Pyramidal π_2	$\langle c+a \rangle$	$\{1\bar{1}22\}[11\bar{2}\bar{3}]$	$\pi_2\langle c+a \rangle$
Tension twin	…	$\{10\bar{1}2\}[\bar{1}011]$	T1
Tension twin	…	$\{11\bar{2}1\}[\bar{1}\bar{1}26]$	T2
Compression twin	…	$\{11\bar{2}2\}[\bar{1}\bar{1}23]$	C1

At each stage of the deformation, individual grains are analysed to obtain information about the glides and/or twin inside individual grain. For each stage of compression, .300 grains are analysed.

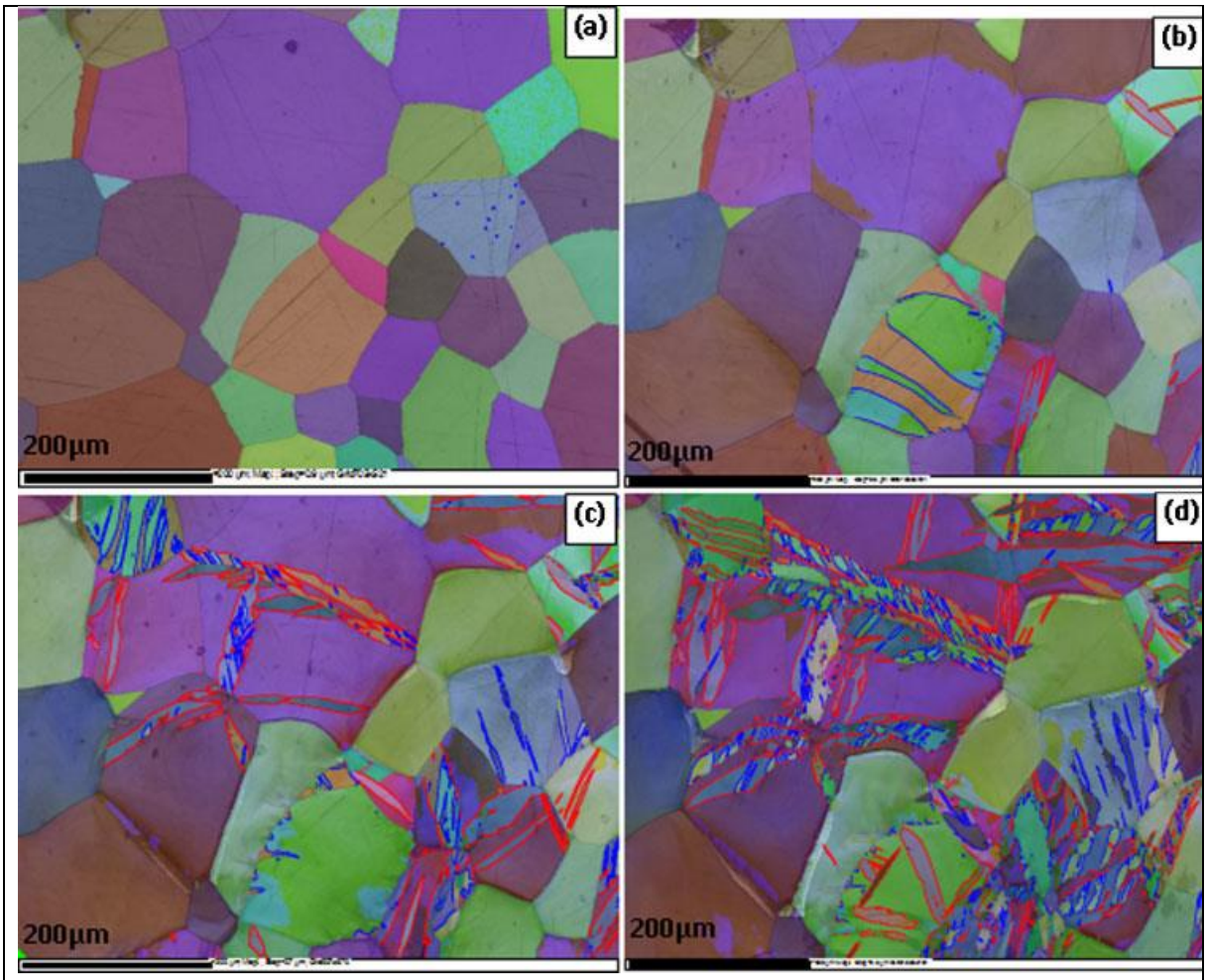

Fig. 3 *Mapping (EBSD) of a undeformed, b 10%, c 20% and d 30% deformed sample*

The variation in different glide systems over the deformation process is shown in Fig. 4. From Fig. 4, it can be seen that initially all the glide systems are of higher amount and progress of deformation it reduces. At the beginning of the deformation process, the growth of twin is not significant, but with higher amount of deformation, twinning makes the disappearance of the glide system. At the initial stage, as all the glide systems have been observed, which is not expected, it therefore becomes obvious to determine the CRSS of different glide systems. An effort has been made to have an idea about the difference of CRSS between prismatic and pyramidal glide systems.

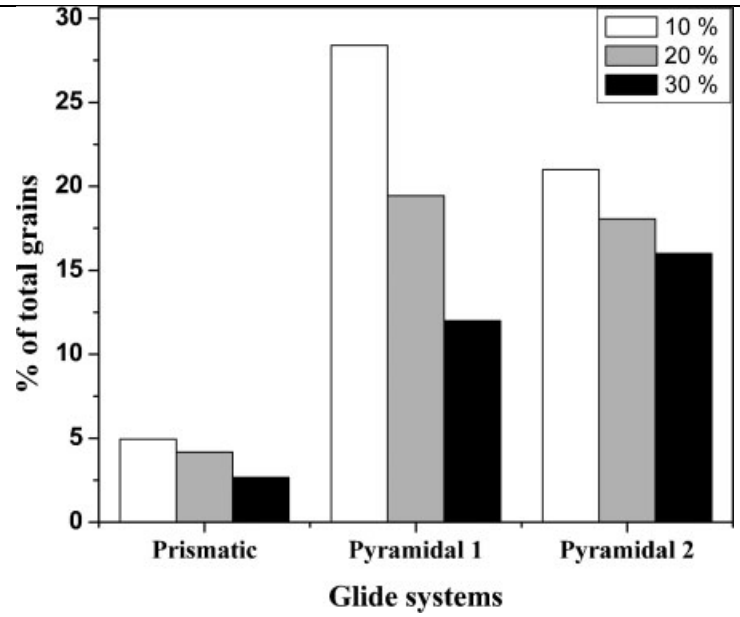

Fig. 4 *Variation in different glide systems with progress of deformation*

When statistical analysis was carried out, the orientations of grains having prismatic slips were differentiated from pyramidal 1 slips. After that, all the orientation results are plotted in a single orientation map. This has become possible only for 10 and 20% compressed samples. For the 30% sample, as the amount of twinned grain is very high, glide system identification was not accurate.

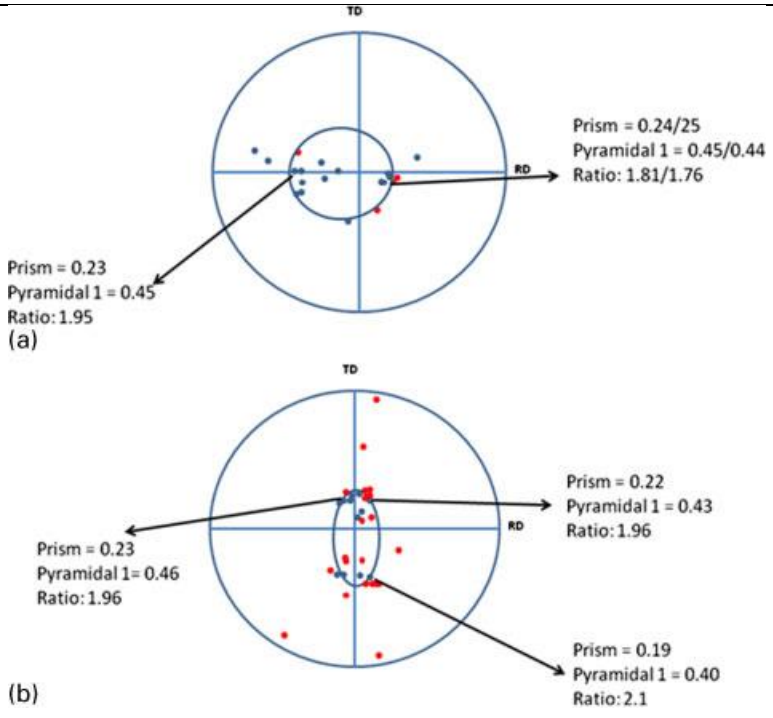

Fig. 5 *Calculation (CRSS) of a 10% and b 20% deformed samples*

The above mentioned plots are shown in Fig. 5. In Fig. 5, the prismatically slipped grains have different domains than that of the pyramidal one.

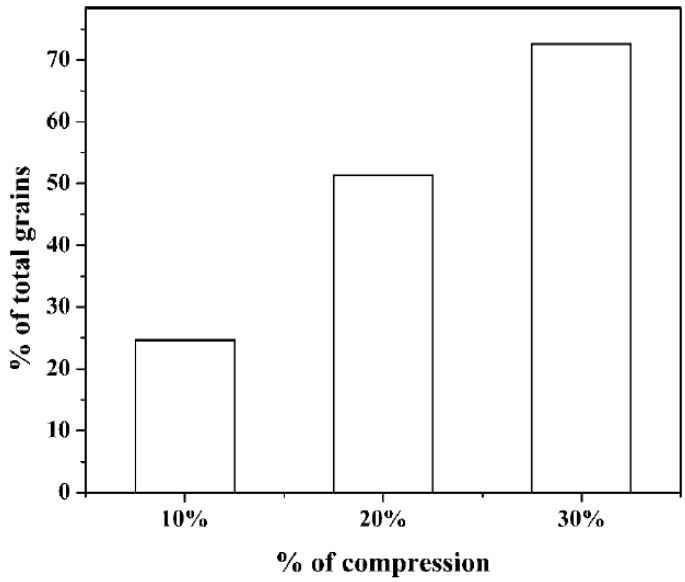

Fig. 6 *Variation in twinned grain with progress of deformation*

There is a distinct boundary observed between these two glide systems. In a few cases at the boundary, a few grains but having different glide systems are observed, and they are marked with arrows in the figure. For those grains, though the orientation is similar, a different slip system is observed inside the grain. As the amount of load applied during deformation and orientation is same for those grains, thus the following equation also holds true there

$$\sigma_{\mathrm{P}} * SF_{\mathrm{P}} = \sigma_{\pi 1} * SF_{\pi 1} \ (\sigma = \mathrm{CRSS}) \qquad (1)$$

The SFs of all the individual grains are captured during the statistical analysis. Therefore, from equation (1), it can be concluded that $\mathrm{CRSS_P/CRSS_{\pi 1}}$=1.8–1.95, which is also indicated in the figure. A similar approach can also be taken to estimate the CRSS of other slip systems, but because of the limited number of data points for them, it restricts further calculations. Therefore, from Fig.5, it can be concluded that as the difference of CRSS is not very high, thus all the glide systems are initiated from the beginning of deformation.

From the statistical analysis, estimation has been made on the twinned grains with progress of deformation.

The result is shown in Fig. 6. It is observed that after 30% deformation, only a few untwinned grains are left. The orientation distribution of the untwinned grains with progress of deformation is shown in Fig. 7. It is found that after 30% deformation, those grains where no twinning is observed belong to the most stable orientation in the hexagonal close packed system. However, the evolution of twins and its mechanism are not under the purview of the present paper. It will be discussed separately.

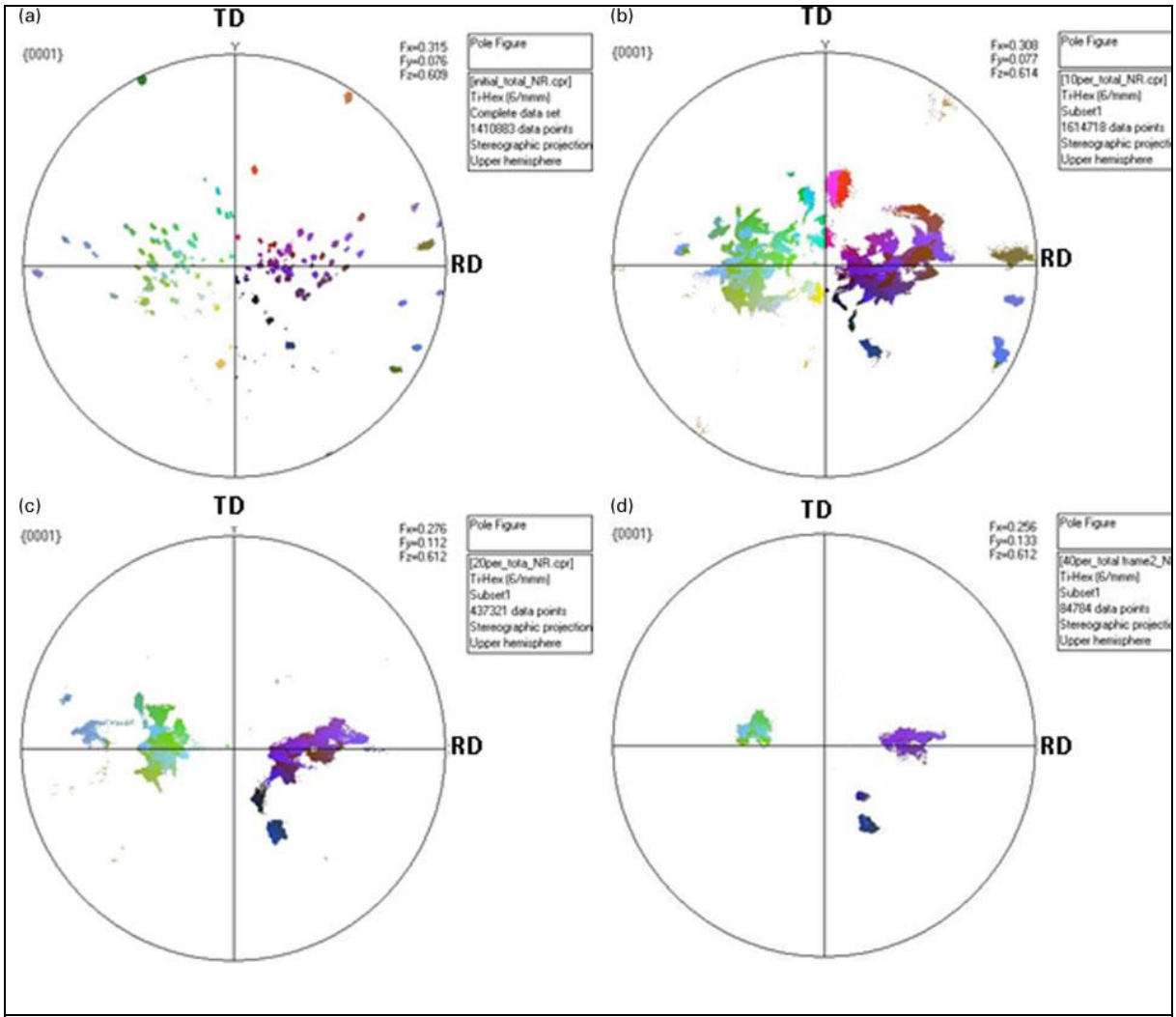

Fig. 7 *Pole figure (0002) of untwinned grains of a undeformed, b 10%, c 20% and d 30% deformed samples*

An effort has been made to determine the glide system other than prismatic by TEM technique. Glide system determination is possible only for 10% deformed sample.

In other cases, the dislocation density is very high; therefore, the glide system determination became an impossible task. However, the TEM results along with the SAD pattern are shown in Fig. 8. From Fig. 6, it is observed that initially for the dark field image, few dislocation lines are observed. For the particular glide system, the *g.b=0* principle is applied, and then the SAD pattern (Fig. 7b) is taken. After the SAD pattern, the sample is tilted by 3.5° using double tilt, and again, the dark field image (Fig. 7c) is taken.

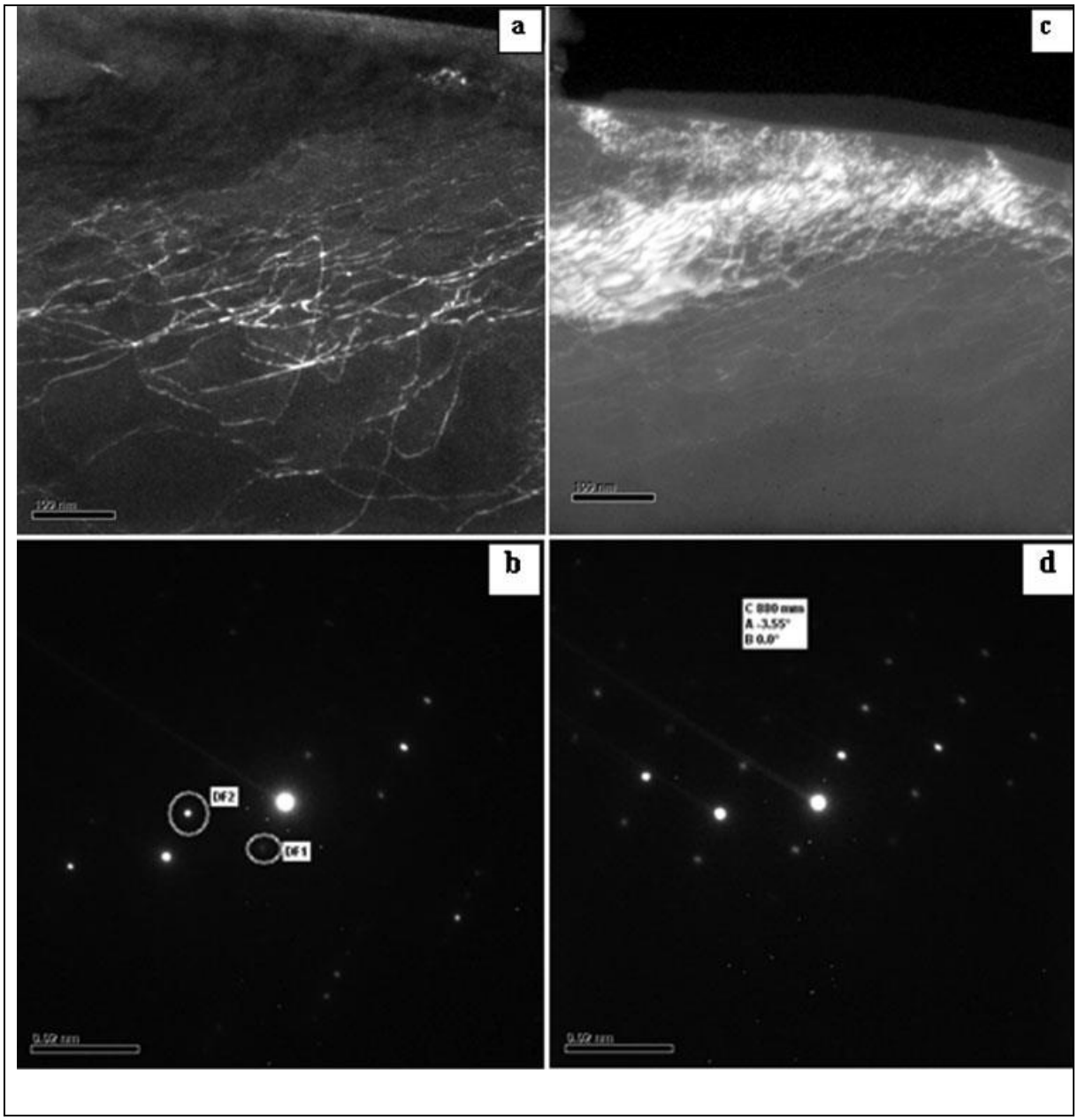

Fig. 8 *a dark filed image showing few dislocation lines, b diffraction pattern of region shown in a, c dark filed image showing after 3?5u rotation and showing disappearance of dislocation lines and d diffraction pattern of region shown in c*

This image shows no dislocation lines, which are observed in Fig. 7a. The SAD pattern also indicates the disappearance of a particular spot. From these two SAD patterns (Fig. 7b and d), a detailed mathematical calculation is made using the crystallography equation. It is found that the glide system is of f11- 01g½112- 0 type, which is nothing but the pyramidal 1<a> type. This method is repeated in a few more grains to confirm the result further.

Conclusions

From the above results and disussion, the following points may be concluded.

1. Prismatic slip is prevalent at the initial stage of deformation.

2. $CRSS_P/CRSS\pi 1=1.8–1.95$.

3. After 30% deformation, ,75% grains are twinned.

4. Twining does not take place in those grains having the most stable orientation as per the hexagonal close packed system.

5. The TEM results confirm the presence of pyramidal slips beside prismatic ones.

Acknowledgement

The present work was supported by the Federation of Research for Aeronautic and Space [Fédération de Recherche pour l'Aéronautique et l'Espace Thème Matériaux pour l'Aéronautique et l'Espace: project optimisation de la mise en forme d'alliage de titane (OPTIMIST)].

References

1. M. J. Philippe, M. Serghat, P. van Houtte and C. Esling: Acta Metall. Mater., 1995, 43, 1619.

2. J. J. Fundenberger, M. J. Philippe, F. Wagner and C. Esling: Acta Mater., 1997, 45, 4041.

3. A. Akhtar: Metall. Mater. Trans. A, 1975, 6A, 1105.

4. P. G. Partridge: Metall Rev., 1967, 12, 169.

5. G. W. Groves and A. Kelly: Philos. Mag., 1963, 8, 877.

6. D. R. Thornburg and H. R. Piehler: 'Titanium science and technology', (ed. R. I. Jaffee and H. M. Burte), Vol. 2, 1187; 1973, New York, Plenum Press.

7. Z. Keshavarz and M. R. Barnett: Scr. Mater., 2006, 55, 915.

8. T. A. Mason, J. F. Bingert, G. C. Kaschner, S. I. Wright and R. J. Larsen: Metall. Mater. Trans. A, 2002, 33A, 949.

9. T.Ung'ar,M.G.Glavicic, L. Balogh,K.Nyilas, A. A. Salem, G.Rib'arik and S. L. Semiatin: Mater. Sci. Eng. A, 2008, A493, 79.

10. S. Zaefferer: Mater. Sci. Eng. A, 2003, A344, 20.

11. J. J. Fundenberger, A. Morawiec, E. Bouzy and J. S. Lecomte: Ultramicroscopy, 2003, 96, 127.

12. J. J. Fundenberger, A. Morawiec, E. Bouzy and J. S. Lecomte: Mater. Chem. Phys., 2003, 81, 535.